Article ID: 1000-324X(2023)01-0055-07 **DOI:** 10.15541/jim20220119

Construction of Prussian Blue Fluorescent Nanoprobe for Specific Detection of HClO in Cancer Cells

DU Qiujing[1,2], LIU Tianzhi[1], CHEN Jufeng[1,2], CHEN Hangrong[1]

(1. State Key Laboratory of High Performance Ceramics and Superfine Microstructures, Shanghai Institute of Ceramics, Chinese Academy of Sciences, Shanghai 200050, China; 2. University of Chinese Academy of Sciences, Beijing 100049, China)

Abstract: Hypochlorous acid (HClO) is one of the reactive oxygen species (ROS), taking crucial parts in many physiological and pathological processes. However, excessive HClO causes tissue injuries, atherosclerosis, neurodegeneration diseases, and even cancers. Therefore, real-time detection of HClO in cancer cells is of importance for exploring the effect of HClO in tumor progression or immunotherapy. Quite different from present organic molecular probes, a novel inorganic-based hydrophilic fluorescent nanoprobe was developed by simply integrating fluorescein isothiocyanate (FITC) into hollow mesoporous Prussian Blue nanoparticles (HMPB) in this work. Owing to inner filter effect, fluorescence of FITC within HMPB quenches to some extent, which can be restored *via* the Fe^{2+}-ClO^{-} redox reaction. A typical fluorescence increase of FITC at emission peak of 520 nm can be clearly observed in the presence of HClO *in vitro*, which exhibits a good linear relationship in the range of 5×10^{-6}–50×10^{-6} mol/L in HClO detection and its detection limit is calculated to be 2.01×10^{-6} mol/L. Furthermore, the cellular experiment demonstrates the specific detection capability of HClO in cancer cells with high sensitivity by the obtained nanoprobe.

Key words: Prussian Blue; fluorescent probe; detection of HClO

Reactive oxygen species (ROS) are highly reactive and short-lived chemical species in living organism, which play a key role in linking fundamental chemistry to intricate physiological and pathological processes[1-5]. Cancer cells are commonly identified with increased ROS level compared to normal cells. Mounting evidences suggest that such intrinsic ROS stress of cancer cells is highly associated with tumor progression[6-9]. However, ROS beyond the threshold level, can also act as an anticancer agent to break the cellular redox homeostasis, resulting in apoptosis[10-11]. Thus, ROS is a double-edged sword for cancer cells. Thereinto, HClO, as one of the most important ROS, can be endogenously generated from hydrogen peroxide and chloride ions with the catalysis of myeloperoxidase enzyme[12]. Generally, HClO is mainly produced by immune cells (*e.g.*, neutrophils, macrophages) as immune defense against invasive pathogens and bacteria. As is known, the immune cells are somehow disabled of its surveillance feature while tumorigenesis happens, and further turn to aid tumor progression while remaining in the tumor microenvironment[13]. Surprisingly, they can still be reactivated of its antitumor effect, known as the popular cancer immunotherapy[14]. Thus, the specific role of HClO in tumor biology or immunotherapy is believed to be vital yet complicated and needs further exploration, which, however, is still in its infancy.

Real-time detection of HClO fluctuation in cancer cells is considered to be the prerequisite for studying its biological effect in malignant tumors. Due to high spatiotemporal resolution of fluorescence imaging, a variety of organic fluorescent probes have been developed for selective imaging of HClO[15-18], most of which are those molecular probes containing HClO-specific redox group (*e.g.*, C＝C double bond, chalcogenide, aldoxime group). The specific HClO-mediated oxidation

Received date: 2022-03-03; **Revised date:** 2022-03-31; **Published online:** 2022-05-09
Foundation item: National Key R&D Program of China (2021YFB3801001); National Natural Science Foundation of China (32030061); The Key Program for Basic Research of Shanghai (19JC1415600).
Biography: DU Qiujing (1997–), female, Master candidate. E-mail: duqiujing19@mails.ucas.ac.cn
杜邱静(1997–), 女, 硕士研究生. E-mail: duqiujing19@mails.ucas.ac.cn
Corresponding author: CHEN Hangrong, professor. E-mail: hrchen@mail.sic.ac.cn
陈航榕, 研究员. E-mail: hrchen@mail.sic.ac.cn

reaction can lead to fluorescence signal alterations of such molecular probes, including “Turn On”, “Turn Off”, “ratiometric”, *etc.*, thus rendering highly sensitive detection or imaging of HClO. However, the construction of these organic probes is generally cumbersome and the existence of carbocyclic structure endows them with poor water solubility, resulting in inhomogeneous distribution in live cells and incomplete reaction with HClO. In addition, these small molecular organic probes also suffer from cell leakage and need binding with larger substrate to avoid efflux[19]. To the best of our knowledge, it is rarely explored of using hydrophilic nanoprobe for fluorescence imaging of HClO *via* the transition metal-mediated redox reaction, which could present a great potential to circumvent the intrinsic drawbacks of organic probes. Prussian Blue (PB), as a typical metal organic frame material, shows excellent performances in wastewater treatment[20], energy storage[21], tumor treatment[22], sensor[23], and other aspects. Recently, PB stands out in biosensing application[24-26], owing to its low toxicity, unique framework structure and easy to be synthesized. For example, a high performance fluorescence switching system triggered electrochemically by Prussian Blue was reported for detecting sulfite[27]. However, there were no more reports for the fluorescent probes based on Prussian Blue for detecting HClO as yet.

Herein, a novel inorganic-organic composite nanoprobe, namely, FITC@HMPB (F@H), was designed by simply loading organic dye into the pores of hollow mesoporous Prussian Blue nanoparticles (HMPB), which presents good dispersion stability without complicated molecular design and covalent attachment in the composite nanoprobe, effectively avoiding disadvantages of pure organic dye probes. Specifically, the HMPB was prepared by polyvinylpyrrolidone (PVP) as protective agent and hydrochloric acid (HCl) as etching agent. The obtained F@H exhibits excellent detection capability of HClO, based on the inner filter effect[28-32]. More details, the excitation or emission light can be absorbed by absorbers when the absorbance spectra of absorbers overlaps with the fluorescence excitation or emission spectra of fluorophores. Owing to the inner filter effect, the fluorescence of FITC within HMPB quenched without HClO. Interestingly, the fluorescence signals could recover accompanied by the degradation of HMPB in the presence of HClO, enabling the real-time detection of HClO in the cancer cells (Fig. 1).

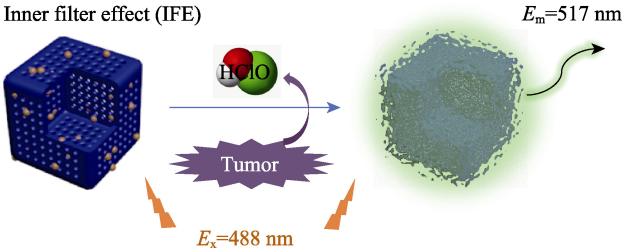

Fig. 1 Illustration of activation mechanism of fluorescence signal when F@H presenting in the HClO

1 Experimental

1.1 Chemicals

All chemicals including potassium ferricyanide ($K_3[Fe(CN)_6]$), polyvinyl pyrrolidone (PVP K30), hydrochloric acid (HCl, 12 mol/L), fluorescein isothiocyanate isomer (FITC), sodium hypochlorite (NaClO, 4%), hydrogen peroxide (H_2O_2, 30%), tert-butyl hydroperoxide (TBHP, 70%) were used without further purification. All reagents mentioned above were purchased from Sinopharm Chemical Reagent Co.. 2,2′-azobis-2-methyl-propanimidamide (AAPH) was obtained from Aladdin, and sodium nitroferricyanide dihydrate (SNP) was purchased from Rhawn. 4T1 cells (mouse breast cancer cells) were obtained from National Collection of Authenticated Cell Culture. Distilled water was used for all experiments.

1.2 Characterization

X-ray diffraction (XRD) patterns of all samples were collected in the range 5°–90°(2θ) using a Rigaku D/max 2550 diffractometer (CuKα radiation, λ=0.15406 nm), operated at 40 kV and 40 mA. Transmission electron microscopy (TEM) images were acquired on a JEM-2100F electron microscope. Dynamic light scattering measurement was conducted on Malvern Zetasizer Nano ZS model ZEN3600 (Worcestershire, UK). UV-Vis-NIR spectra were recorded on a UV-3101PC shimadzu spectroscope. X-ray photoelectron spectrum (XPS) was obtained on a Thermo ESCALAB 250Xi X-ray photoelectron spectrometer. The fluorescence spectra were recorded on a Shimadzu RF-5301 PC spectrophotometer. The CLSM images were collected by using FV 1000 system (Olympus Company, Japan).

1.3 Preparation of F@H probe

Prussian Blue nanoparticles and hollow mesoporous Prussian Blue nanoparticles were synthesized *via* a modified hydrothermal method according to our previous report [33]. Afterwards, 5 mg of HMPB were dispersed in 5 mL distilled water *via* sonication. Then, 1 mg of FITC was added in the above HMPB dispersion, and the obtained mixture was placed in the incubating shaker at a constant temperature of 37 ℃ overnight. Afterwards, the FITC@HMPB (F@H) was obtained *via* centrifugation and washed with distilled water once. Finally, the obtained F@H was redispersed in 5 mL distilled water for further use.

1.4　Detection of HClO

The F@H was dispersed in Tris-HCl buffer (pH 5.5) to obtain the stock suspension. Then the HClO was added into the stock solution to gain 2 mL of mixed solution, which contains 50 μg/mL of F@H and different concentrations of HClO (0–50 μmol/L). After incubation for 2 min, fluorescence spectra were obtained with excitation wavelength of arround 488 nm. All procedures were conducted at room temperature.

1.5　Cytotoxicity

4T1 cells were seeded into a 96-well culture plate at a density of 5000 cells/well and left to adherence in a cell culture incubator for 12 h. The as-prepared F@H with various concentrations (0, 12.5, 25, 50, 100 μg/mL, n=6) in cell culture medium DMEM containing 10% fetal bovine serum (FBS) were added into the above culture plate. The corresponding cell viability was measured by a standard CCK-8 reduction assay (Cell Counting Kit, Dojindo Laboratories, Kumamoto, Japan).

1.6　Confocal imaging of 4T1 cells

4T1 cells were cultured on the 6-well cell culture plate with 14 mm glass coverslips and allowed to incubate for 24 h, followed by washing with phosphate buffer solution (PBS) three times. After that, cells in blank group were incubated in DMEM without serum while cells in negative control and experimental groups were incubated with F@H (50 μg/mL) in DMEM without serum. All groups were incubated for 2 h at 37 ℃ in a 5%CO_2/95% air incubator in this step. After incubation, cells were washed three times with PBS. For detecting exogenous HClO, the experimental group was treated with 100 μmol/L NaClO for 0.5 h in DMEM without serum at 37 ℃, while the other groups were treated by DMEM without serum and NaClO. For detecting endogenous HClO, the experimental group was treated with 50 μmol/L elescolmol in DMEM without serum at 37 ℃ while the other groups were treated by DMEM without serum and elescolmol for 0.5 h.

2　Results and discussions

2.1　Characterization of HMPB

TEM image (Fig. 2(a)) shows that the prepared HMPB displays high dispersion with average size of arround 160 nm. The dynamic light scattering result indicates that the suspension containing 50 μg/mL of HMPB in Tris-HCl keeps high dispersion with narrow size distribution of 190 nm in diameter even after 12 h (Fig. S1), indicating that HMPB is of great dispersion stability. XRD pattern (Fig. 2(b)) confirms the single crystal structure of HMPB with good crystallinity. N_2 adsorption-desorption analysis result (the inset of Fig. 2(c)) indicates that the specific surface area and pore volume of HMPB are 124 m^2/g and 0.56 cm^3/g, respectively, with a homogeneous mesopore of 3.2 nm. This hollow mesoporous structure endows HMPB with high loading efficiency. More details, the maximum loading amount of FITC is 14.4% and encapsulation rate is 83.9% (Fig. S2 and Table S1). Notably, the loading amount of FITC could be controlled *via* different feed ratios, nevertheless, the loading amount of FITC affects little to the sensitivity or stability of the fluorescent probe.

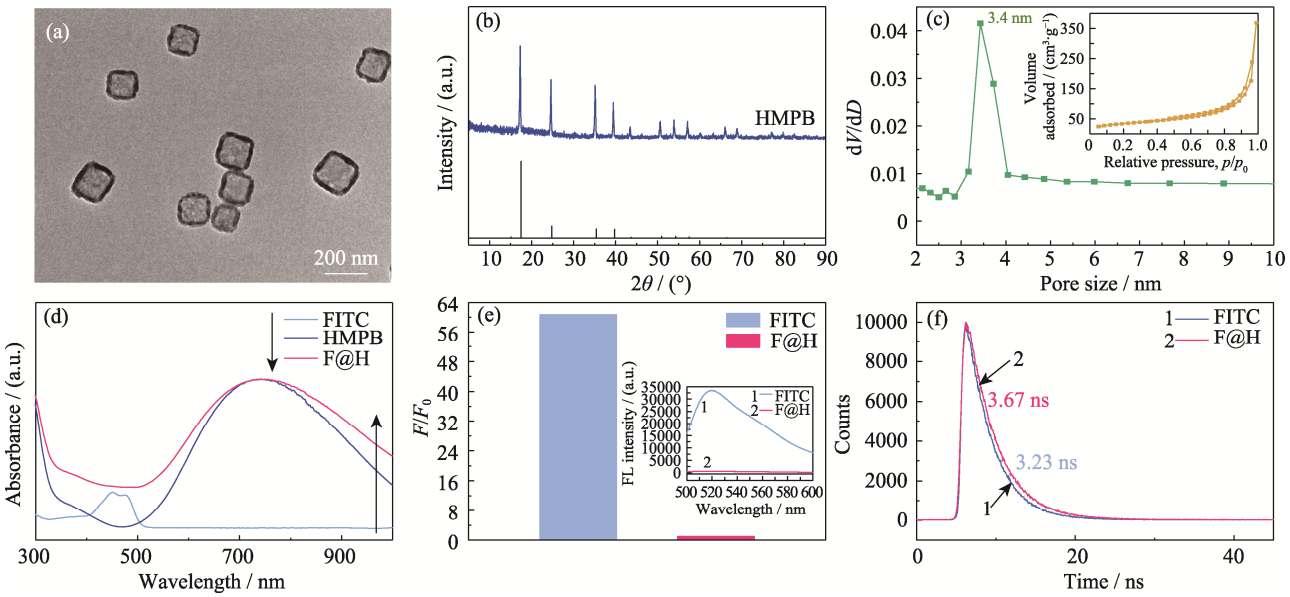

Fig. 2　Characterization of the prepared HMPB and F@H

(a) Typical TEM image, (b) XRD pattern, and (c) pore-size distribution curve of HMPB with inset showing N_2 adsorption-desorption isotherm; (d) UV-Vis spectra of FITC, HMPB and F@H; (e) Fluorescence spectra of free FITC and F@H with inset showing corresponding fluorescence intensity ratio at 520 nm; (f) Fluorescence life of FITC and F@H

UV-Vis spectra shown in the Fig.2 (d) indicate that free FITC presents an obvious adsorption peak at 488 nm, and the absorbance peak at around 750 nm is ascribed to HMPB. It is interesting to find that the obtained F@H shows the same absorbance peak at 750 nm, meanwhile, the intensity at 488 nm, was obviously enhanced, implying the successful loading of FITC into HMPB. It is worth noting that the fluorescence intensity at emission peak (520 nm) of FITC sharply decreased after loading into HMPB (Fig. 2(e)). To explore this interesting phenomenon, the fluorescence life was tested. As shown in Fig. 2(f), F@H shows almost the same fluorescence lifetime as FITC, confirming the existence of inner filter effect between HMPB and FITC.

2.2 *In vitro* detection of HClO and mechanism

Afterwards, the *in vitro* detection capability of the probe in aqueous solution was studied. As shown in Fig. 3(a), it is clearly found that the fluorescence intensity at emission peak of 520 nm gradually increases with the addition of HClO to F@H suspension. The detection limit could be calculated to be 2.01 μmol/L according to the linear relationship between fluorescence intensity at 520 nm and HClO concentration within the range of 0 to 50 μmol/L (Fig. 3(b)). Fig. 3(c) shows the change of absorbance of F@H before and after addition of NaClO, indicating that HMPB could react with HClO within 1 min, in accordance with the fluorescence responsive time (within 2 min, Fig. S3), suggesting quick response and high sensitivity of the obtained probe. Furthermore, the electronic states and chemical composition of HMPB before and after addition of NaClO were measured by X-ray photoelectron spectroscope (XPS). As shown in Fig. 3(d), the peaks located at 708.6 and 709.6 eV are assigned to the binding energy of $Fe2p_{3/2}$ of HMPB with the valence state of Fe^{2+} and Fe^{3+}, respectively. It is noting to find that after addition of NaClO, the ratio Fe^{2+}/Fe^{3+} of peak area decreases from 1 to 0.72, which results from that HMPB is oxidized by ClO^-.

Furthermore, the specificity of F@H probe for HClO under the same analytical conditions was tested. As shown in Fig. 3(a), it is found that the fluorescence of F@H presents negligible changes in the presence of other ROS (TBHP, ROO·, NO, H_2O_2, ·OH, $ONOO^-$), even at high concentration (500 μmol/L). Moreover, the UV-Vis spectra (Fig. 3(b)) also indicate that HMPB could not react with other ROS species. Thus the obtained F@H nanoprobe exhibits outstanding selectivity to HClO.

2.3 Imaging of HClO in living cancer cells

Before investigation on the applicability of the prepared F@H probe to detect HClO in living cells, the cytotoxicity of F@H was assessed by 2-(2-methoxy-4-nitrophenyl)-3-(4-nitrophenyl)-5-(2, 4-disulfonic acid benzene)-2h-tetrazole monosodium salt (CCK-8) analysis

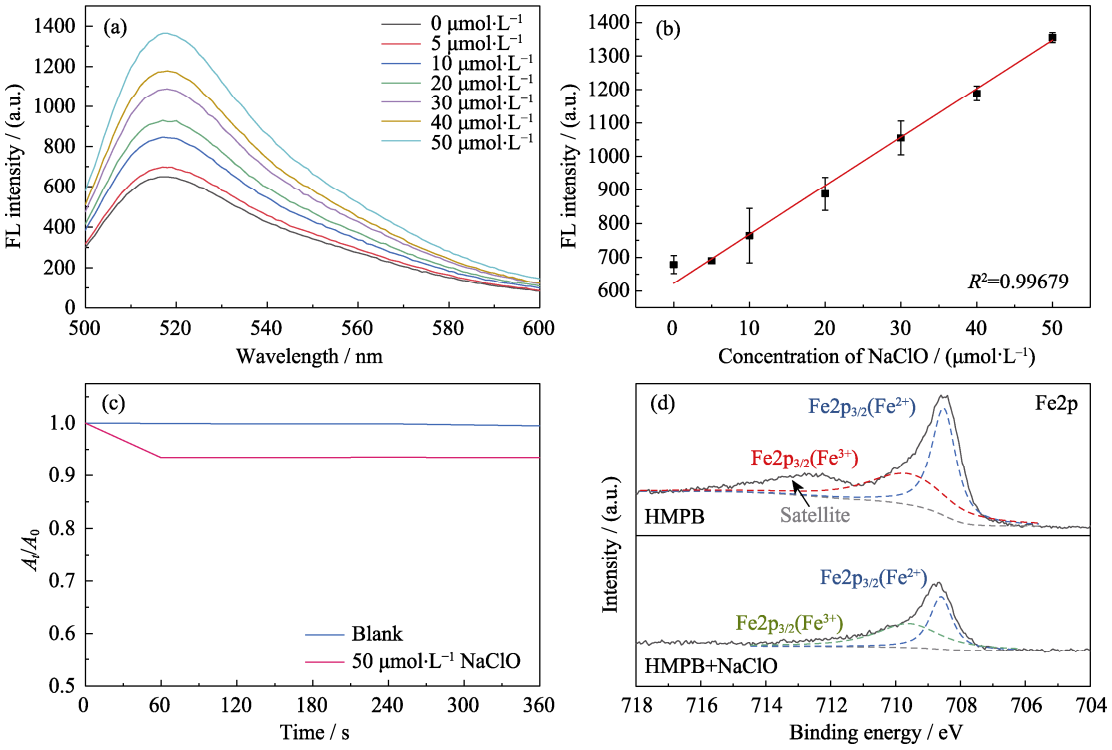

Fig. 3 *In vitro* detection of HClO and mechanism

(a, b) Fluorescence (FL) spectra (a) and the corresponding calibration curve (b) of F@H (50 μg/mL) with the addition of NaClO (0–50 μmol/L) in Tris-HCl (10 mmol/L, pH 5.5). λ_{ex}=488 nm, λ_{em}=520 nm; (c) Absorbance of F@H varied with time before and after addition of NaClO; (d) XPS profiles of F@H without/with addition of NaClO

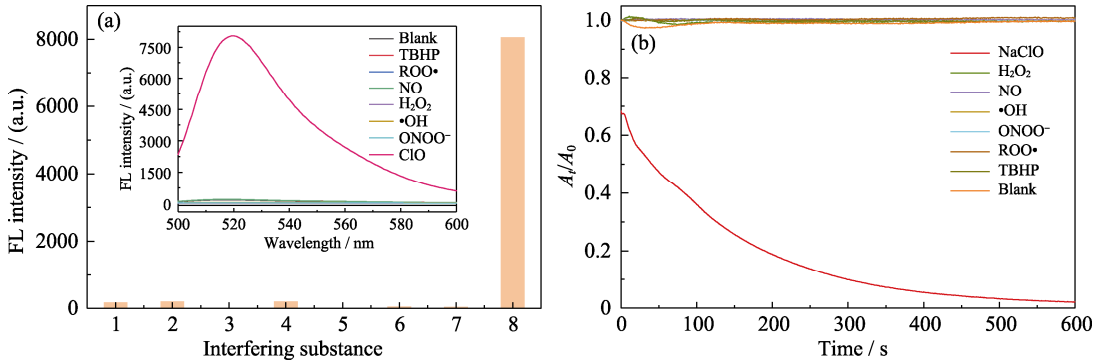

Fig. 4　Fluorescence of F@H in the presence of other ROS

(a) Fluorescence spectra (inset of (a)) and the corresponding fluorescence (FL) intensity (a) of F@H (50 μg/mL) with the addition of different interfering substances (500 μmol/L, 1-blank, 2-TBHP, 3-ROO, 4-NO, 5-H_2O_2, 6-·OH, 7-$ONOO^-$, 8-ClO^-) in Tris-HCl (10 mmol/L, pH 5.5) λ_{ex}=488 nm, λ_{em}=520 nm; (b) Absorbance change of F@H with addition of different interfering substances (500 μmol/L)

Colorful figures are available on website

in 4T1 cells. The results indicate that the prepared F@H shows good cytocompatibility with almost no toxicity (Fig. S4).

Afterwards, the confocal fluorescence imaging of different groups were conducted in cellular level for comparison. As shown in Fig. 5, for the control group, *i.e.*, F@H-pretreated 4T1 cells without addition of NaClO or elesclomol, the 4T1 cells incubated with F@H (50 μg/mL) for 2.5 h showed weak fluorescence under excitation. In contrast, for the NaClO group, after further added NaClO (100 μmol/L) into F@H and co-cultured with 4T1 cells for another 30 min, much enhanced fluorescence was clearly observed, indicating that the F@H probe was capable of detecting exogenous HClO in living cells.

To confirm the capability detection of endogenous HClO, elesclomol, an experimental ROS-generating anticancer agent[34], was used as a model drug to induce the endogenous production of HClO in 4T1 cells in this study. In the elesclomol group, the F@H-pretreated 4T1 cells were co-incubated with 50 μmol/L elesclomol, and the fluorescence imaging was recorded at 0.5 h (Fig. 5(c, d, g–i)). It is found that the fluorescence signal of elesclomol group shows significant increase at 30 min, which is ascribed to the endogenous generation of HClO in 4T1 cells induced by elesclomol. This result also indicates that the F@H can be used to monitor the cellular oxidative stress.

3　Conclusion

In brief, a novel fluorescent probe based on hollow mesoporous Prussian Blue nanoparticles was developed *via* a facile method without complex fluorescent molecular design, for the first time, to achieve the rapid and specific detection of HClO with high sensitivity. More details, FITC molecular confined inside the mesoporous channel of HMPB induces the fluorescence quenching owing to the inner filter effect. Significantly, the fluorescence signal of FITC can be restored accompanied by degradation of HMPB in the presence of HClO. The obtained F@H presents a high signal-to-noise ratio with response time within 2 min and the detection limit is calcaulted to be 2.01 μmol/L. More importantly, it can be

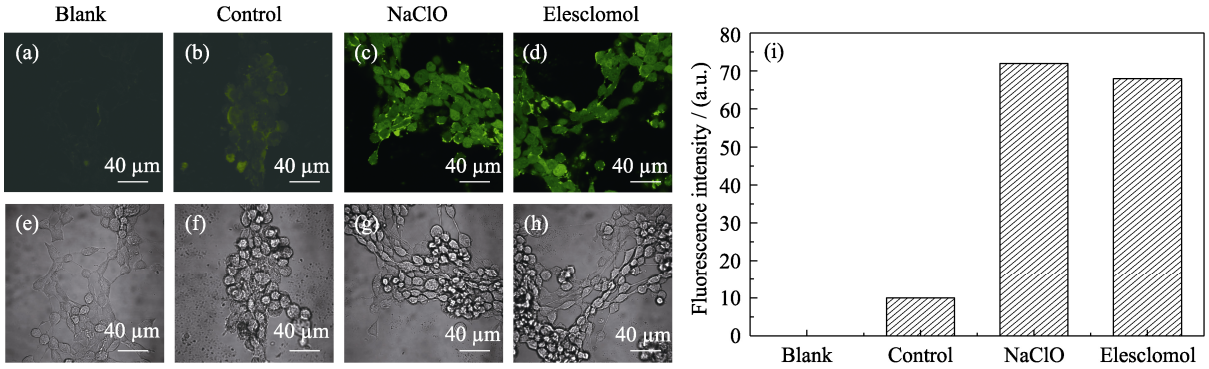

Fig. 5　Detecting HClO in living cancer cells

(a-d) Confocal fluorescence and (e-h) bright field images for detecting exogenous or endogenous HClO in 4T1 cells Blank: without any treatments; Control: 50 μg/mL of F@H and 0 μmol/L NaClO; NaClO: 50 μg/mL of F@H and 100 μmol/L NaClO; Elesclomol: 50 μg/mL of F@H and 50 μmol/L elesclomol. λ_{ex}=488 nm, λ_{em}=520 nm; (i) Statistical analyses of the confocal images

further used to detect the endogenous HClO of tumor cells and monitor the elevation of HClO in 4T1 cells induced by elesclomol. Overall, this study demonstrated a new fluorescence detection method using inorganic nanoparticles as responsive carrier, providing a promising detection strategy for HClO in tumor tissue.

Supporting Materials:

Supporting Materials related to this article can be found at https://doi.org/10.15541/jim20220119.

References:

[1] DICKINSON B, CHANG C. Chemistry and biology of reactive oxygen species in signaling or stress responses. *Nature Chemical Biology*, 2011, **7(8):** 504.

[2] CHEN X, WANG F, HYUN J, *et al.* Recent progress in the development of fluorescent, luminescent and colorimetric probes for detection of reactive oxygen and nitrogen species. *Chemical Society Reviews*, 2016, **45(10):** 2976.

[3] CHEN X, TIAN X, SHIN I, *et al*. Fluorescent and luminescent probes for detection of reactive oxygen and nitrogen species. *Chemical Society Reviews*, 2011, **40(9):** 4783.

[4] LOU Z, LI P, HAN K. Redox-responsive fluorescent probes with different design strategies. *Accounts of Chemical Research*, 2015, **48(5):** 1358.

[5] LIPPERT A R, BITTNER G, CHANG C. Boronate oxidation as a bioorthogonal reaction approach for studying the chemistry of hydrogen peroxide in living systems. *Accounts of Chemical Research*, 2011, **44(9):** 793.

[6] SCHUMACKER P T. Reactive oxygen species in cancer cells: live by the sword, die by the sword. *Cancer Cell*, 2006, **10(3):** 175.

[7] TOYOKUNI S, OKAMOTO K, YODOI J, *et al.* Persistent oxidative stress in cancer. *FEBS Letters*, 1995, **358(1):** 1.

[8] HILEMAN E, LIU J, ALBITAR M, *et al*. Intrinsic oxidative stress in cancer cells: a biochemical basis for therapeutic selectivity. *Cancer Chemotherapy and Pharmacology*, 2004, **53(3):** 209.

[9] BEHREND L, HENDERSON G, ZWACKA R. Reactive oxygen species in oncogenic transformation. *Biochemical Society Transactions*, 2003, **31(6):** 1441.

[10] KONG Q, LILLEHEI K. Antioxidant inhibitors for cancer therapy. *Medical Hypotheses*, 1998, **51(5):** 405.

[11] KONG Q, BEEL J, LILLEHEI K. A threshold concept for cancer therapy. *Medical Hypotheses*, 2000, **55(1):** 29.

[12] KLEBANOFF S. Myeloperoxidase: friend and foe. *Journal of Leukocyte Biology*, 2005, **77(5):** 598.

[13] SCHREIBER R, OLD L, SMYTH M. Cancer immunoediting: integrating immunity's roles in cancer suppression and promotion. *Science*, 2011, **331(6024):** 1565.

[14] PAGGIO J. Cancer immunotherapy and the value of cure. *Nature Reviews Clinical Oncology*, 2018, **15(5):** 268.

[15] GAO W, MA Y, LIU Y, *et al.* Observation of endogenous HClO in living mice with inflammation, tissue injury and bacterial infection by a near-infrared fluorescent probe. *Sensors and Actuators B: Chemical,* 2021, **327:** 128884.

[16] MA H, CHEN K, SONG B, *et al.* A visible-light-excitable mitochondria-targeted europium complex probe for hypochlorous acid and its application to time-gated luminescence bioimaging. *Biosensors and Bioelectronics*, 2020, **168:** 112560.

[17] LUO P, ZHAO X. A sensitive and selective fluorescent probe for real-time detection and imaging of hypochlorous acid in living cells. *ACS Omega*, 2021, **6(18):** 12287.

[18] MA Q, WANG C, BAI Y, *et al*. A lysosome-targetable and ratiometric fluorescent probe for hypochlorous acid in living cells based on a 1, 8-naphthalimide derivative. *Spectrochimica Acta Part A: Molecular and Biomolecular Spectroscopy*, 2019, **223:** 117334.

[19] YU F, DU T, WANG Y, *et al.* Ratiometric fluorescence sensing of UiO-66-NH_2 toward hypochlorite with novel dual emission *in vitro* and *in vivo*. *Sensors and Actuators B: Chemical*, 2022, **353:** 131032.

[20] FAUSTINOA P, YANG S, PROGAR J, *et al*. Quantitative determination of cesium binding to ferric hexacyanoferrate: Prussian Blue. *Journal of Pharmaceutical and Biomedical Analysis*, 2008, **47(1):** 114.

[21] YOU Y, WU X, YIN Y, *et al.* High-quality Prussian Blue crystals as superior cathode materials for room-temperature sodium-ion batteries. *Energy & Environmental Science*, 2014, **7(5):** 1643.

[22] HOU L, GONG X, YANG J, *et al*. Hybrid-membrane-decorated Prussian Blue for effective cancer immunotherapy *via* tumor-associated macrophages polarization and hypoxia relief. *Advanced Materials*, 2022, **34(14):** 2200389.

[23] RICCI F, MOSCONE D, TUTA C, *et al*. Novel planar glucose biosensors for continuous monitoring use. *Biosensors and Bioelectronics*, 2005, **20(10):** 1993 .

[24] PAZ E, BARFIDOKHT A, RIOS S, *et al*. Extended noninvasive glucose monitoring in the interstitial fluid using an epidermal biosensing patch. *Analytical Chemistry*, 2021, **93(37):** 12767.

[25] SEMPIONATTO J, MOON J, WANG J. Touch-based fingertip blood-free reliable glucose monitoring: personalized data processing for predicting blood glucose concentrations. *ACS Sensor*, 2021, **6(5):** 1875.

[26] KARPOVA E, SHCHERBACHEVA E, GALUSHIN A, *et al*. Noninvasive diabetes monitoring through continuous analysis of sweat using flow-through glucose biosensor. *Analytical Chemistry,* 2019, **91(6):** 3778.

[27] ZHAI Y, ZHANG H, ZHANG L, *et al*. A high performance fluorescence switching system triggered electrochemically by Prussian Blue with upconversion nanoparticles. *Nanoscale*, 2016, **8(18):** 9493.

[28] XU C, ZHOU Y, ZHOU Y, *et al*. A facile ratiometric sensing platform based on inner filter effect for hypochlorous acid detection. *Sensors and Actuators B: Chemical,* 2020, **325:** 128766.

[29] HAN L, LIU S, LIANG J, *et al*. pH-mediated reversible fluorescence nanoswitch based on inner filter effect induced fluorescence quenching for selective and visual detection of 4-nitrophenol. *Journal of Hazardous Materials*, 2019, **362:** 45.

[30] ZHANG Q, SUN Y, LIU M, *et al*. Selective detection of Fe^{3+} ions based on fluorescence MXene quantum dots *via* a mechanism integrating electron transfer and inner filter effect. *Nanoscale*, 2020, **12(3):** 1826.

[31] YAN F, ZU F, XU J, *et al.* Fluorescent carbon dots for ratiometric detection of curcumin and ferric ion based on inner filter effect, cell imaging and PVDF membrane fouling research of iron flocculants in wastewater treatment. *Sensors and Actuators B: Chemical*, 2019, **287:** 231.

[32] LIU H, XU C, BAI Y, *et al*. Interaction between fluorescein isothiocyanate and carbon dots: inner filter effect and fluorescence resonance energy transfer. *Spectrochimica Acta Part A: Molecular and Biomolecular Spectroscopy*, 2017, **171:** 311,

[33] CAI X, GAO W, MA M, *et al*. A Prussian Blue-based core-shell hollow-structured mesoporous nanoparticle as a smart theranostic agent with ultrahigh pH-responsive longitudinal relaxivity.

Advanced Materials, 2015, **27(41):** 6382.
[34] KIRSHNER J, HE S, BALASUBRAMANYAM V, *et al*. Elesclomol induces cancer cell apoptosis through oxidative stress. *Molecular Cancer Therapeutics*, 2008, **7(8):** 2319.

普鲁士蓝基 HClO 荧光纳米探针及其对肿瘤细胞的特异性检测

杜邱静[1,2], 刘天智[1], 陈菊锋[1,2], 陈航榕[1]

(1. 中国科学院 上海硅酸盐研究所, 上海 200050; 2. 中国科学院大学, 北京 100049)

摘 要: 次氯酸(HClO)是一种活性氧(ROS), 在许多生理和病理过程中起着至关重要的作用。然而, 过量的 HClO 会导致组织损伤、动脉粥样硬化、神经退行性疾病甚至癌症。因此, 实时检测肿瘤细胞中 HClO 对于探索 HClO 在肿瘤进展以及免疫治疗中的作用具有重要意义。与目前常用的工艺复杂、水溶性差的有机分子探针不同, 本工作简单地将异硫氰酸荧光素(FITC)与中空介孔普鲁士蓝纳米粒子(HMPB)相结合, 构建了一种新型的无机亲水荧光纳米探针。由于内滤光效应, HMPB 中 FITC 的荧光有一定程度的猝灭, 但通过 Fe^{2+}-ClO^-氧化还原反应可恢复荧光。 体外条件下, 加入 HClO 后, FITC 在发射峰(520 nm)处荧光逐渐增强, HClO 在 5×10^{-6}~50×10^{-6} mol/L 范围内呈良好的线性关系, 检出限为 2.01×10^{-6} mol/L。此外, 在细胞水平上, 该纳米探针对癌细胞中的 HClO 显示出良好的特异检测能力, 且灵敏度高。

关　键　词: 普鲁士蓝; 荧光探针; HClO 检测

中图分类号: TQ138　　**文献标志码:** A

Supporting Materials:

Construction of Prussian Blue Fluorescent Nanoprobe for Specific Detection of HClO in Cancer Cells

DU Qiujing[1,2], LIU Tianzhi[1], CHEN Jufeng[1,2], CHEN Hangrong[1]

(1. State Key Laboratory of High Performance Ceramics and Superfine Microstructures, Shanghai Institute of Ceramics, Chinese Academy of Sciences, Shanghai 200050, China; 2. University of Chinese Academy of Sciences, Beijing 100049, China)

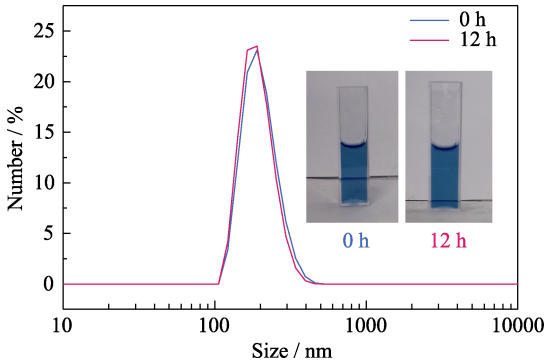

Fig. S1 Dynamic light scattering (DLS) result of HMPB with insets showing digital photographs of HMPB suspension standing still for 0 and 12 h.

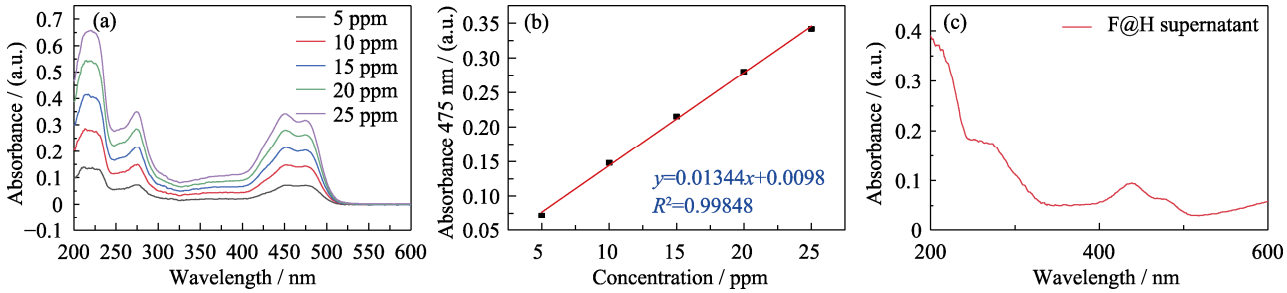

Fig. S2 Standard curves (a) and the corresponding calibration curve (b) of FITC, UV-Vis spectrum of F@H supernatent (c)
ppm: μg/mL

Table S1 Calculated encapsulation efficiency and loading efficiency by the standard curve and UV-Vis spectrum of F@H supernatant

Encapsulation Efficiency	83.9%
Loading Efficiency	14.4%

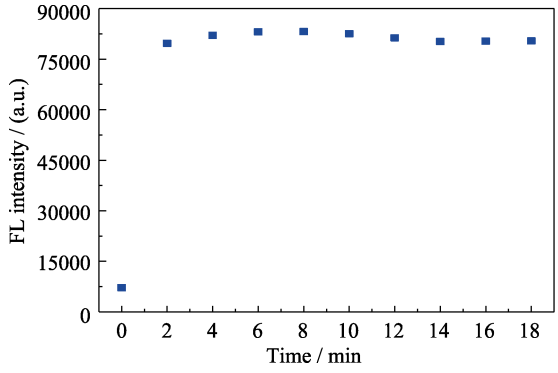

Fig. S3 Time-dependent fluorescence intensity of F@H (50 μg/mL) upon the addition of 50 μmol/L NaClO in Tris-HCl buffer (10 mmol/L, pH=5.5). λ_{ex} = 488 nm, λ_{em} = 520 nm.

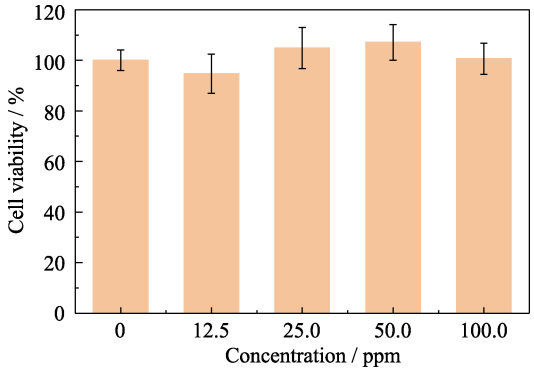

Fig. S4 Cytotoxicity of F@H on 4T1 cells. Cells were incubated with 0–100 μmol/L F@H in DMEM medium containing 10% fetal bovine serum (FBS) for 24 h.
ppm: μg/mL